CANCER

Reduced abundance of the E3 ubiquitin ligase E6AP contributes to decreased expression of the *INK4/ARF* locus in non–small cell lung cancer

Cristina Gamell,[1,2] Twishi Gulati,[1,2] Yaara Levav-Cohen,[3] Richard J. Young,[4] Hongdo Do,[5] Pat Pilling,[6] Elena Takano,[7] Neil Watkins,[8] Stephen B. Fox,[7] Prudence Russell,[9] Doron Ginsberg,[10] Brendon J. Monahan,[11] Gavin Wright,[12,13] Alex Dobrovic,[5] Sue Haupt,[1,2] Ben Solomon,[2,4] Ygal Haupt[1,2,14,15]*

The tumor suppressor p16^{INK4a}, one protein encoded by the *INK4/ARF* locus, is frequently absent in multiple cancers, including non–small cell lung cancer (NSCLC). Whereas increased methylation of the encoding gene (*CDKN2A*) accounts for its loss in a third of patients, no molecular explanation exists for the remainder. We unraveled an alternative mechanism for the silencing of the *INK4/ARF* locus involving the E3 ubiquitin ligase and transcriptional cofactor E6AP (also known as UBE3A). We found that the expression of three tumor suppressor genes encoded in the *INK4/ARF* locus (*p15^{INK4b}*, *p16^{INK4a}*, and *p19^{ARF}*) was decreased in *E6AP$^{-/-}$* mouse embryo fibroblasts. E6AP induced the expression of the *INK4/ARF* locus at the transcriptional level by inhibiting *CDC6* transcription, a gene encoding a key repressor of the locus. Luciferase assays revealed that E6AP inhibited *CDC6* expression by reducing its E2F1-dependent transcription. Chromatin immunoprecipitation analysis indicated that E6AP reduced the amount of E2F1 at the *CDC6* promoter. In a subset of NSCLC samples, an E6AP-low/CDC6-high/p16^{INK4a}-low protein abundance profile correlated with low methylation of the gene encoding p16^{INK4a} (*CDKN2A*) and poor patient prognosis. These findings define a previously unrecognized tumor-suppressive role for E6AP in NSCLC, reveal an alternative silencing mechanism of the *INK4/ARF* locus, and reveal E6AP as a potential prognostic marker in NSCLC.

INTRODUCTION

The genes within the *INK4/ARF* locus encode the key tumor suppressors p15^{INK4b}, p16^{INK4a}, and alternate reading frame (ARF) (p14^{ARF} in humans and p19^{ARF} in mice). A loss of the *INK4/ARF* locus is among the most frequent events in human cancer (*1*, *2*). P15^{INK4b} and p16^{INK4a} bind to and inhibit cyclin-dependent kinase 4 (CDK4) and CDK6, causing hypophosphorylation of retinoblastoma protein (pRb) and cell cycle arrest, whereas ARF activates p53 by protecting it from mouse double minute 2 homolog (MDM2)–mediated degradation (*3*). Hence, the gene products of the *INK4/ARF* locus control the two main tumor suppressor pathways in the cell, the ARF-p53 and the p16^{INK4a}-pRb pathways. The *INK4/ARF* locus is a sensor of oncogenic stress, becoming transcriptionally activated by aberrant proliferating signals, such as those generated by RAS and MYC (*2*). Gene expression from the *INK4/ARF* locus is controlled at multiple levels by a myriad of mechanisms, which involve interplay between positive and negative regulators. The behavior of the locus suggests the existence of regulatory elements with capacity to exert a global effect on the entire *INK4/ARF* locus. For example, epigenetic regulation of the entire *INK4/ARF* locus by the Polycomb repressive complexes (PRC1 and PRC2) is well established, where various Polycomb group (PcG) proteins, such as BMI-1, can repress the entire locus (*3*). The *INK4/ARF* locus can also be regulated at the transcriptional level by cell division control protein 6 (CDC6). Binding of CDC6 to the cis-acting upstream regulatory domain of *INK4/ARF* represses the whole locus through recruitment of histone deacetylases and increased methylation of histone H3 on lysine 9 (H3K9), which are hallmarks of heterochromatinization (*4*). CDC6 itself is a replication licensing factor, which is transcriptionally activated by the transcription factor E2F1 in a cell cycle–coordinated manner (*5*, *6*). Consistent with its ability to repress the *INK4/ARF* locus, CDC6 is increased in abundance in a number of human cancers such as non–small cell lung cancer (NSCLC) (*7*–*9*), mantle cell lymphoma (*10*), oral squamous cell carcinoma (*11*), cervical cancer (*12*, *13*), and prostate cancer (*14*). Moreover, common regulatory domain deletions have been identified in multiple human cell lines and pheochromocytoma tumors (*15*).

The protein E6AP (also known as UBE3A) has been extensively studied in a neurodevelopmental condition known as Angelman syndrome (*16*) and in the context of human papillomavirus (HPV)–induced cervical carcinogenesis. In the latter, its interaction with HPV E6 oncoprotein drives the ubiquitination and degradation of p53 (*17*). Beyond HPV-induced cancer, E6AP has been linked to breast cancer (*18*), prostate cancer (*19*, *20*), and B cell lymphoma (*21*). E6AP emerges as a key E3 ubiquitin ligase capable of regulating several molecules important in cancer including p53 (*22*–*24*), promyelocytic leukemia protein (PML) (*25*), and p27 (*26*). Beyond its E3 ligase activity, E6AP can also act as a transcriptional cofactor, with the best-characterized targets being the nuclear hormone receptors

[1]Tumour Suppression Laboratory, Peter MacCallum Cancer Centre, Melbourne, Victoria 3000, Australia. [2]Sir Peter MacCallum Department of Oncology, University of Melbourne, Victoria 3000, Australia. [3]The Hebrew University Hadassah Medical School, Jerusalem 9112102, Israel. [4]Molecular Therapeutics and Biomarkers Laboratory, Peter MacCallum Cancer Centre, Melbourne, Victoria 3000, Australia. [5]Translational Genomics and Epigenomics Laboratory, Olivia Newton-John Cancer Research Institute, Melbourne, Victoria 3084, Australia. [6]Biomedical Manufacturing Program, Commonwealth Scientific and Industrial Research Organization, Melbourne, Victoria 3169, Australia. [7]Department of Pathology, Peter MacCallum Cancer Centre, Melbourne, Victoria 3000, Australia. [8]The Kinghorn Cancer Centre, Garvan Institute of Medical Research, Darlinghurst, New South Wales 2010, Australia. [9]Department of Anatomical Pathology, St. Vincent's Hospital, Melbourne, Victoria 3065, Australia. [10]The Mina and Everard Goodman Faculty of Life Sciences, Bar-Ilan University, Ramat-Gan 5290002, Israel. [11]Systems Biology and Personalised Medicine, Walter and Eliza Hall Institute of Medical Research, Melbourne, Victoria 2555, Australia. [12]Department of Surgery, St. Vincent's Hospital, Melbourne, Victoria 3065, Australia. [13]Division of Cancer Surgery, Peter MacCallum Cancer Centre, Melbourne, Victoria 3000, Australia. [14]Department of Biochemistry and Molecular Biology, Monash University, Melbourne, Victoria 3800, Australia. [15]Department of Pathology, University of Melbourne, Victoria 3800, Australia. *Corresponding author. Email: ygal.haupt@petermac.org

(*27*, *28*). We have uncovered a novel role of E6AP in the regulation of cellular senescence in mouse embryonic fibroblasts (MEFs) under oxidative or oncogenic (HRAS) stress conditions in vivo and in vitro (*29*, *30*). In the search for the molecular mechanism by which E6AP suppresses cancer, we examined the effect of E6AP on the *INK4/ARF* locus as a major regulatory node of multiple tumor-suppressive pathways.

RESULTS

Loss of E6AP reduces gene expression of the *INK4/ARF* locus

We have previously shown that *E6AP*-null (*E6AP*$^{-/-}$) MEF cells bypass replicative and oncogene-induced senescence (*29*, *30*). Because p16^{INK4a} is a key regulator of cellular senescence (*2*, *3*), we examined the effect of E6AP on p16^{INK4a} abundance. A comparison of early-passage *E6AP*$^{-/-}$ MEFs and their wild-type counterparts showed a marked reduction in p16^{INK4a} protein abundance (Fig. 1A). To verify that the observed differences were due to *E6AP* expression and not due to spontaneous immortalization of the MEFs, we reconstituted *E6AP*$^{-/-}$ MEFs with E6AP using a retroviral vector. E6AP overexpression correlated with an increase in p16^{INK4a} protein abundance (Fig. 1B), demonstrating that the effect of E6AP deficiency on reduction of p16^{INK4a} abundance is specific to *E6AP* loss rather than a secondary adaptation of cells due to some other genomic alteration.

We next sought to determine how E6AP regulates p16^{INK4a} expression. As the expression of the genes within the *INK4/ARF* locus is regulated largely at the transcriptional level (*2*, *3*), we analyzed the mRNA expression of *p15*^{INK4b} (*CDKN2B*), *p16*^{INK4a} (*CDKN2A*), and *p19*^{ARF} (ARF product of the *CDKN2A* locus) in the E6AP$^{-/-}$ MEFs. Markedly, *E6AP*$^{-/-}$ MEFs showed significantly lower mRNA expression of all the *INK4/ARF* genes (Fig. 1C), in particular, that of *p16*^{INK4a}. These results support a role for E6AP in the regulation of the entire *INK4/ARF* locus.

Loss of E6AP suppresses the *INK4/ARF* locus through induction of CDC6 expression

To further explore the effect of E6AP in the *INK4/ARF* locus regulation, we analyzed the effect of E6AP presence on key proteins implicated in epigenetic and transcriptional silencing of the locus. We focused our attention on the proteins encoded by the PcG genes and on *CDC6* because of their documented ability to silence the entire *INK4/ARF* locus (*3*). We detected no significant alteration in the abundance of key PcG proteins (BMI-1, CBX2, MEL18, and RING1B) in *E6AP*$^{-/-}$ MEFs cells relative to wild-type cells (Fig. 2A), whereas CDC6 abundance was clearly increased (Fig. 2B), suggesting that the ability of *E6AP*$^{-/-}$ MEF cells to bypass senescence might depend preferentially on *CDC6* up-regulation. Reconstitution of E6AP expression in *E6AP*$^{-/-}$ MEFs reduced the abundance of CDC6 (Fig. 2C), further supporting the specificity of the effect of E6AP on CDC6 abundance.

Because E6AP acts as an E3 ubiquitin ligase and as a transcription cofactor, we next investigated at what level E6AP regulates *CDC6* expression. To analyze whether E6AP affects CDC6 at the protein level, we treated *E6AP*$^{-/-}$ and wild-type MEFs with cycloheximide to block protein synthesis and subsequently measured CDC6 abundance at different time points. Consistent with our data above (Fig. 2B), the basal abundance of CDC6 was greater in *E6AP*$^{-/-}$ MEFs than in wild-type MEFs; however, the half-life of CDC6 protein was not affected in the absence of E6AP (Fig. 2D). This suggested that E6AP does not affect CDC6 protein stability. Consistent with this notion, *E6AP*$^{-/-}$ and wild-type MEFs showed no differential accumulation of CDC6 protein when treated with the proteasome inhibitor MG132 (Fig. 2E). In contrast, *CDC6* mRNA expression was significantly increased in *E6AP*$^{-/-}$ MEFs compared with wild-type MEFs (Fig. 2F), suggesting that E6AP regulates CDC6 at the transcriptional level. However, we did not detect a difference in *CDC6* transcript stability between wild-type and *E6AP*$^{-/-}$ MEFs cultured with the transcription inhibitor actinomycin D (fig. S1), supporting our conclusion that E6AP regulates CDC6 protein abundance by inhibiting its transcription.

E6AP represses CDC6 expression by inhibiting E2F1 transcriptional activity

CDC6 transcription is induced by the E2F1 transcription factor (*5*); therefore, we sought to test whether E6AP reduced CDC6 abundance by inhibiting E2F1-dependent transcription. First, we measured the effect of E6AP on E2F1-mediated induction of the *CDC6* promoter using a luciferase gene reporter assay. Because E2F1 is tightly regulated by the pRb (*31*), we used Saos-2 cells, which lack pRb expression due to a deletion. Cells were transfected with a CDC6 promoter construct containing the E2F1 binding region (*5*) together with E2F1 and E6AP. E2F1-dependent luciferase activity was reduced by E6AP expression (Fig. 3A and fig. S2), strongly supporting a role for E6AP in repressing *CDC6* expression by inhibiting E2F1-dependent transcription. The possibility that E6AP promotes the degradation of E2F1, thereby impairing the induction of CDC6 expression, was ruled out, as E6AP had no measurable effect on E2F1 protein expression (Fig. 3B). Consistently, we found that the E3 ligase activity of E6AP was not required to repress E2F1-dependent transcription of CDC6 because expression of a catalytically inactive mutant of E6AP (E6AP-C820A) in Saos-2 repressed *CDC6* transcription to a similar extent as did expression of wild-type E6AP (fig. S3). To gain further insight into the mechanism underpinning E6AP regulation of E2F1 transcription activity, we next examined whether E6AP and E2F1 interact. Using coimmunoprecipitation assays in Saos-2 cells, we found an interaction between ectopically expressed E2F1 and endogenous E6AP using an E6AP antibody (Fig. 3C) and between the two endogenous proteins

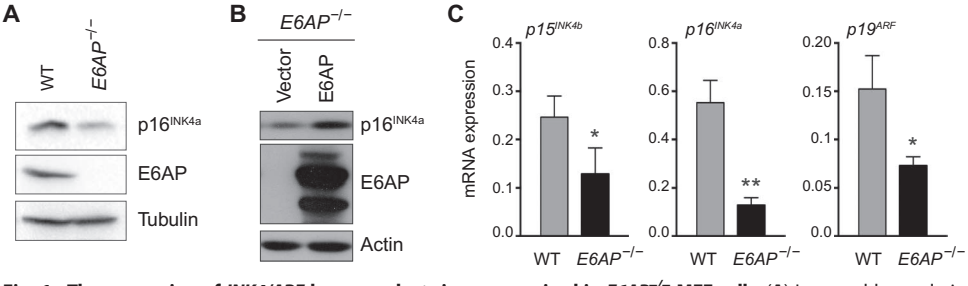

Fig. 1. The expression of *INK4/ARF* locus products is compromised in *E6AP*$^{-/-}$ MEF cells. (**A**) Immunoblot analysis of p16^{INK4a} abundance in early-passage wild-type (WT) and *E6AP*$^{-/-}$ MEFs. (**B**) Analysis of p16^{INK4a} in early-passage *E6AP*$^{-/-}$ MEFs reconstituted with E6AP or empty vector. Blots in (A) and (B) are representative of three independent experiments. (**C**) Reverse transcription polymerase chain reaction (RT-PCR) analysis of the expression of *p15*^{INK4b} (*Cdkn2B*), *p16*^{INK4a} (*Cdkn2A*), and *p19*^{ARF} (*Cdkn2A*) mRNA, normalized to the housekeeping gene *Ubc*. Data are $\Delta\Delta C_t$ ± SD of three independent paired experiments. *P < 0.05, **P < 0.01, unpaired Student's t test.

using an E2F1 antibody (Fig. 3D). Furthermore, we detected E2F1-E6AP complexes in an in vitro coimmunoprecipitation assay using purified proteins (Fig. 3E), indicating that this interaction is direct. We next investigated whether E6AP inhibits the binding of E2F1 to the *CDC6* promoter using chromatin immunoprecipitation (ChIP) analysis in Saos-2 cells with normal or deficient abundance of E6AP. Inducible knockdown of E6AP increased the extent of E2F1 binding to the *CDC6* promoter (Fig. 3F), suggesting that E6AP inhibits E2F-dependent transcription of CDC6 by reducing E2F1 binding to its target genes promoters.

To further interrogate the role of E6AP in E2F1 regulation, we examined whether the effect of E6AP on E2F1 is specific to the *CDC6* promoter or more generally affecting E2F1 transcriptional activity. Using qRT-PCR, we found that the expression of five other E2F1 target genes (*Ccne1*, *Ccnd1*, *Puma*, *Lmnb1*, and *Mcm3*) was increased in *E6AP*$^{-/-}$ MEFs relative to that in wild-type cells (Fig. 4A). This effect of E6AP was selective for E2F1 target genes because the analysis of four non-E2F1 target genes showed no change in expression in *E6AP*$^{-/-}$ MEFs relative to wild-type cells (fig. S4). This result suggested that E6AP inhibits E2F1 activity more broadly, reminiscent of the inhibitory effect of pRb (*31*). To test this notion, we used a luciferase reporter assay to compare *CDC6* expression driven by an E2F1 mutant that cannot be bound by pRb (*32*). We observed that whereas pRb, as expected, was incapable of efficiently inhibiting mutant E2F1-dependent transcription of *CDC6*, E6AP repressed mutant and wild-type E2F1 similarly (Fig. 4B), indicating that E6AP and pRb do not share a binding site on E2F1. However, a competition assay with purified proteins revealed that a truncated form of pRb containing the minimum region shown to repress growth suppression (*33*) competed with E6AP for E2F1 binding in a dose-dependent manner (Fig. 4C, left). Consistent with this result, high amounts of E6AP displaced pRb from its binding to E2F1 (Fig. 4C, right). To better understand the biological implication of the physical interaction between E6AP and E2F1, we used a series of truncated Myc-tagged mutants of E2F1 to map the E6AP binding region. E2F1 wild type and the truncated mutants were in vitro translated in the presence of S35M or S35C mutations, and the lysates were incubated with E6AP to allow binding to occur. An E6AP cocktail of antibodies was used to capture E6AP and coprecipitate any bound complexes. E6AP bound to all E2F1 mutants except the mutant lacking the N-terminal domain (E2F1 ΔN) (Fig. 4D), indicating that the first 198 amino acids of E2F1 were essential to bind E6AP. To corroborate this, we translated nonlabeled

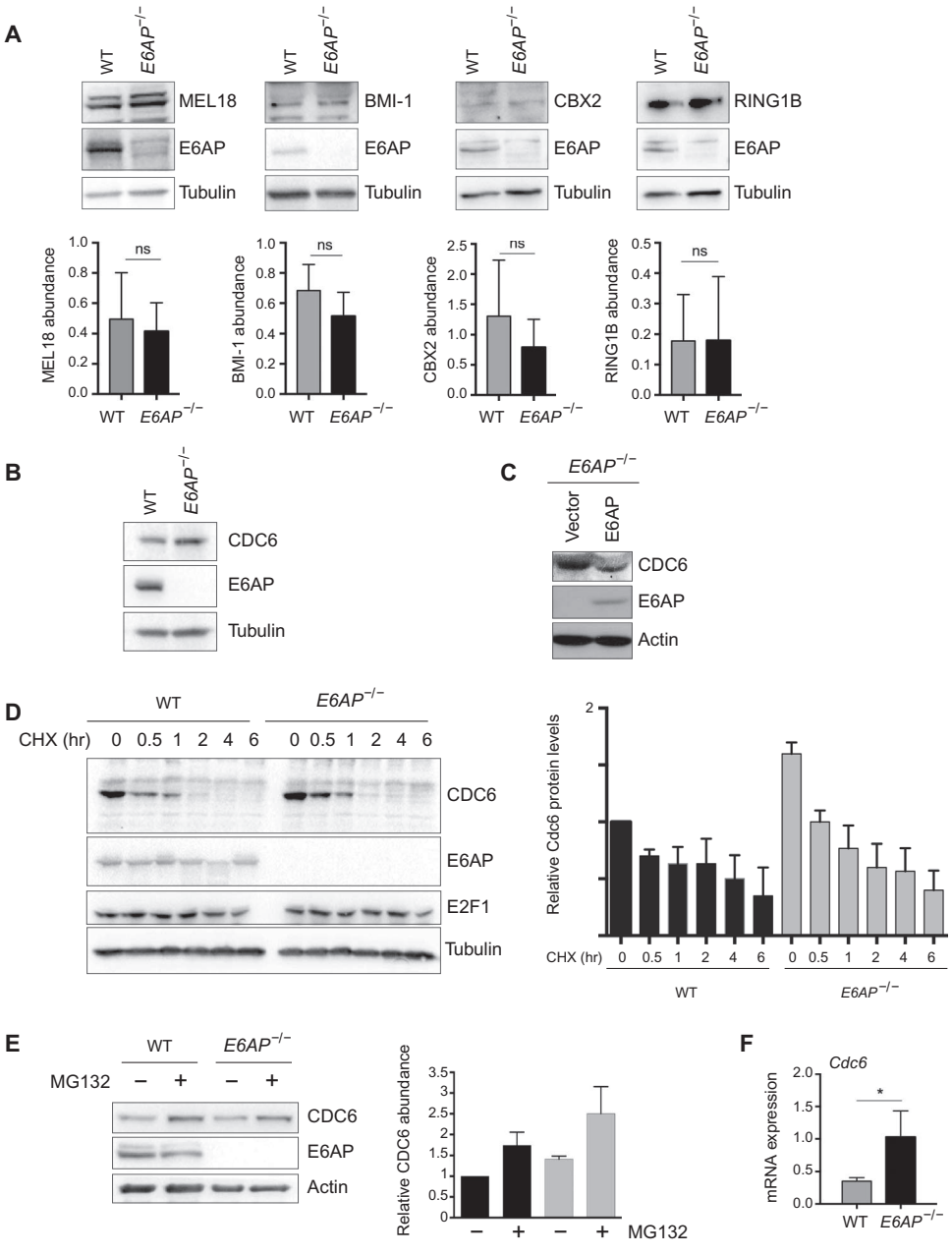

Fig. 2. E6AP stimulates the expression of the *INK4/ARF* locus through repression of CDC6. (**A**) Immunoblot analysis of key PcG proteins in early-passage WT and *E6AP*$^{-/-}$ MEFs. The graphs show the densitometry analysis of three independent experiments. Data are means ± SD. ns, not significant. (**B**) Immunoblot analysis of CDC6 abundance in early-passage WT and *E6AP*$^{-/-}$ MEFs. (**C**) Analysis of CDC6 abundance in early-passage *E6AP*$^{-/-}$ MEFs reconstituted with E6AP. Blots in (B) and (C) are representative of three independent experiments. (**D**) Immunoblot analysis of CDC6 protein stability in WT and *E6AP*$^{-/-}$ MEFs treated with cycloheximide (CHX; 50 μg/ml) or dimethyl sulfoxide (DMSO) (0). Right: Graph of the densitometry analysis from three independent experiments. Data are means ± SEM. hr, hours. (**E**) Immunoblot analysis of CDC6 abundance in WT and *E6AP*$^{-/-}$ MEFs treated with the proteasome inhibitor MG132 (20 μM for 4 hours) or DMSO (–). The graph on the right shows the densitometry analysis of four independent experiments. Data are means ± SEM. (**F**) Quantitative RT-PCR (qRT-PCR) for *Cdc6* mRNA expression, normalized to the housekeeping gene *Ubc*. Data are $\Delta\Delta C_t$ ± SD from six experiments. *P < 0.05, unpaired Student's t test.

Myc-tagged truncated mutants of E2F1 in vitro, and we used anti-Myc antibody to capture E2F1 and measured the amount of E6AP in the immune complexes by immunoblot analysis of E6AP. Consistent with the first approach, E2F1 ΔN failed to complex with E6AP (fig. S5), further supporting the notion that E6AP binds to the first 198 N-terminal amino acids of E2F1. These results strongly suggested that E6AP binds the N-terminal region of E2F1. Overexpression of E6AP and pRb simultaneously repressed E2F1 transcriptional activity to a similar level as each of them individually, indicating that E6AP and pRb have neither a synergistic nor an additive effect on E2F1 activity (fig. S6).

E6AP abundance is down-regulated in a proportion of NSCLC patients, and this correlates with low p16^{INK4a} in tumors and worse overall survival in patients

The results described so far demonstrated a novel link between E6AP and p16^{INK4a} via CDC6 regulation. p16^{INK4a} is frequently silenced in NSCLC patients (*34*–*36*), but only a proportion of these cases (~37%) can be explained by its promoter hypermethylation (*37*). In addition, CDC6 overexpression has been linked to poor prognosis and chemoresistance in NSCLC (*7*–*9*). We therefore hypothesized that the E6AP-CDC6-p16^{INK4a} regulatory axis may provide a molecular explanation for the silencing of p16^{INK4a}, which is not achieved by promoter hypermethylation. To explore this notion, we analyzed the correlation between E6AP, CDC6, and p16^{INK4a} abundance in a clinical setting. Immunohistochemical analysis of a set of tissue microarrays (TMAs) from 185 human resected NSCLC cases with low amounts of p16^{INK4a} revealed a subpopulation of tumors characterized by E6AP-low/CDC6-high/p16^{INK4a}-low, which accounted for 18% of the total NSCLC samples analyzed (95% confidence interval, 13 to 24%) (Fig. 5A). The subpopulation of E6AP-high/CDC6-low/p16^{INK4a}-low cases served as a control group. Consistent with our data showing that E6AP had no effect on E2F1 protein abundance (Fig. 3B), a comparative immunohistochemical analysis of E2F1 protein abundance between E6AP-low/CDC6-high/p16^{INK4a}-low and E6AP-high/CDC6-low/p16^{INK4a}-low subpopulations revealed no difference (fig. S7).

Because DNA hypermethylation is a major known mechanism that silences p16^{INK4a} in NSCLC, we compared the methylation status of the *CDKN2A* promoter (driving p16^{INK4a} expression) between these two groups of tumors. Only 15.3% of the patients in the E6AP-low/CDC6-high/p16^{INK4a}-low group were methylated, as compared with 37.5% in the control group (Fig. 5B). This observation suggested that E6AP-low/CDC6-high–mediated repression of p16^{INK4a} might represent a novel methylation-independent mechanism for p16^{INK4a} silencing in NSCLC.

Querying our data set of NSCLC patients, we observed that patients with E6AP-low/CDC6-high/p16^{INK4a}-low protein expression profile presented significantly reduced overall survival (185 patients, $P = 0.037$) (Fig. 5C). Because sample size limitations precluded clinical subtype–specific analyses of this expression pattern, we evaluated the prognostic value of E6AP in a large publically available clinical data set of lung tumors from 1926 patients (Kaplan-Meier Plotter database). The prognostic power of E6AP was high for stage I (653 patients, $P = 1.4 \times 10^{-5}$) and stage II patients (320 patients, $P = 0.043$) (Fig. 5D), but, as is commonly observed with cancer biomarkers, it was not significant for stage III patients (fig. S8). These analyses support a tumor-suppressive role for E6AP in NSCLC, where patients with low E6AP transcript abundance have significantly reduced overall survival than those with high amounts of E6AP at the early stage of their disease.

We next assessed whether *E6AP* expression had prognostic power in all cases of NSCLC or in any particular histological subtype. The most common NSCLC cancer histological subtypes are

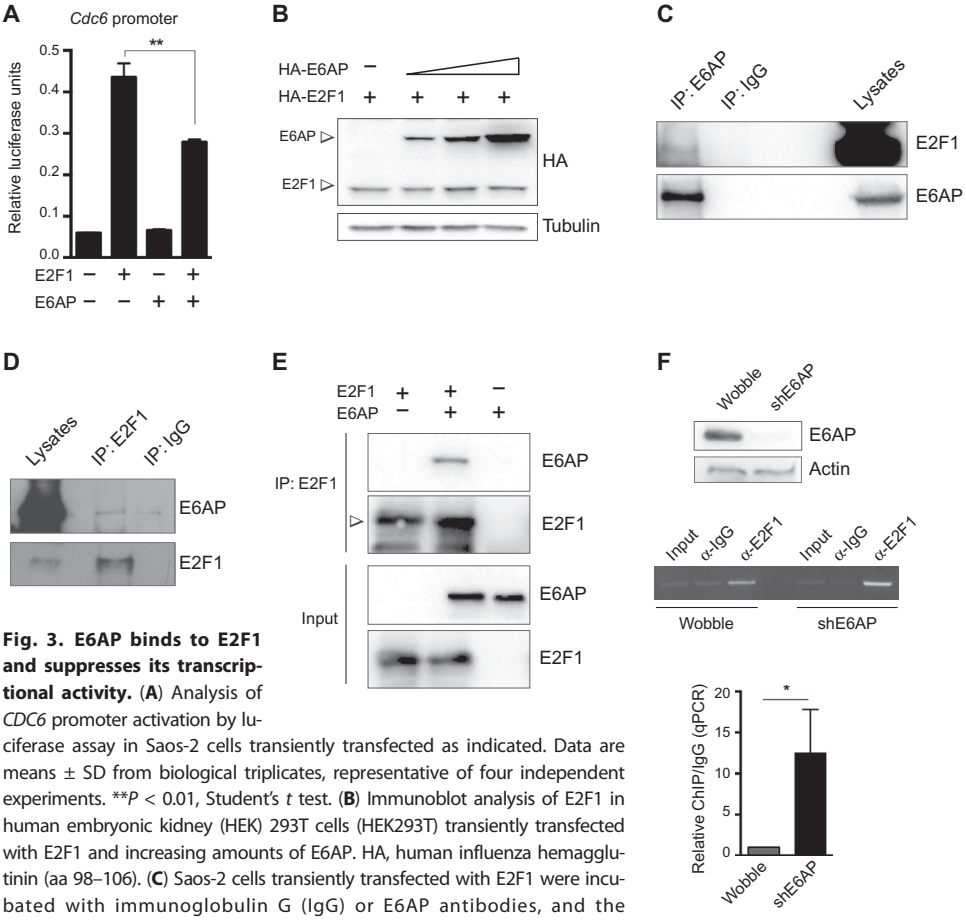

Fig. 3. E6AP binds to E2F1 and suppresses its transcriptional activity. (**A**) Analysis of *CDC6* promoter activation by luciferase assay in Saos-2 cells transiently transfected as indicated. Data are means ± SD from biological triplicates, representative of four independent experiments. $^{**}P < 0.01$, Student's *t* test. (**B**) Immunoblot analysis of E2F1 in human embryonic kidney (HEK) 293T cells (HEK293T) transiently transfected with E2F1 and increasing amounts of E6AP. HA, human influenza hemagglutinin (aa 98–106). (**C**) Saos-2 cells transiently transfected with E2F1 were incubated with immunoglobulin G (IgG) or E6AP antibodies, and the immunoprecipitated proteins (IP) and total cell extracts (lysates) were analyzed by immunoblotting. (**D**) Saos-2 cells were incubated with IgG or E2F1 antibodies, and the immunoprecipitants and input lysates were analyzed by immunoblotting. (**E**) Immunoblot analysis of in vitro coimmunoprecipitation of purified E6AP and E2F1 to assess direct interaction. Arrowhead marks the intended signal. Blots in (B), (C), (D), and (E) are representative of three independent experiments. (**F**) Efficiency of E6AP knockdown (top blot) and ChIP for E2F1 binding to the *CDC6* promoter (lower blot) in Saos-2 cells transduced with inducible shE6AP or wobble control and treated with doxycycline for 4 days. The graph represents the ChIP-qPCR analysis of E2F1 binding to the *CDC6* promoter in the presence (gray bar; Wobble) and absence of E6AP (black bar; shE6AP). Data are means ± SD from three independent experiments. $^{*}P < 0.05$.

adenocarcinoma and squamous cell carcinoma. These two subtypes not only present distinct histological features but also differ in their molecular drivers, pathogenesis, and disease progression, and they require differential treatment strategies. The prognostic power of *E6AP* was further increased in adenocarcinoma patients (865 patients; HR, 0.56; $P = 8.6 \times 10^{-7}$, log-rank), whereas *E6AP* abundance did not correlate with prognosis in squamous cell carcinoma patients (676 patients; HR, 0.89; $P = 0.33$, log-rank) (Fig. 5E), suggesting a clinical subtype–specific role of E6AP. To further validate the contribution of E6AP in patients with lung adenocarcinoma, we analyzed the correlation between E6AP and activating mutations of the KRAS oncogene, which represent the most frequent alteration in human lung adenocarcinomas (~33% of the patients) but are rare in squamous cell carcinoma patients (*38*, *39*). We found that E6AP-low/CDC6-high/p16^{INK4a}-low expression pattern correlated with KRAS mutations in 27% of cases as compared with only 8% in the control population (Fig. 4F), further suggesting that the E6AP/CDC6/p16^{INK4a} axis plays a crucial role in NSCLC adenocarcinoma patients.

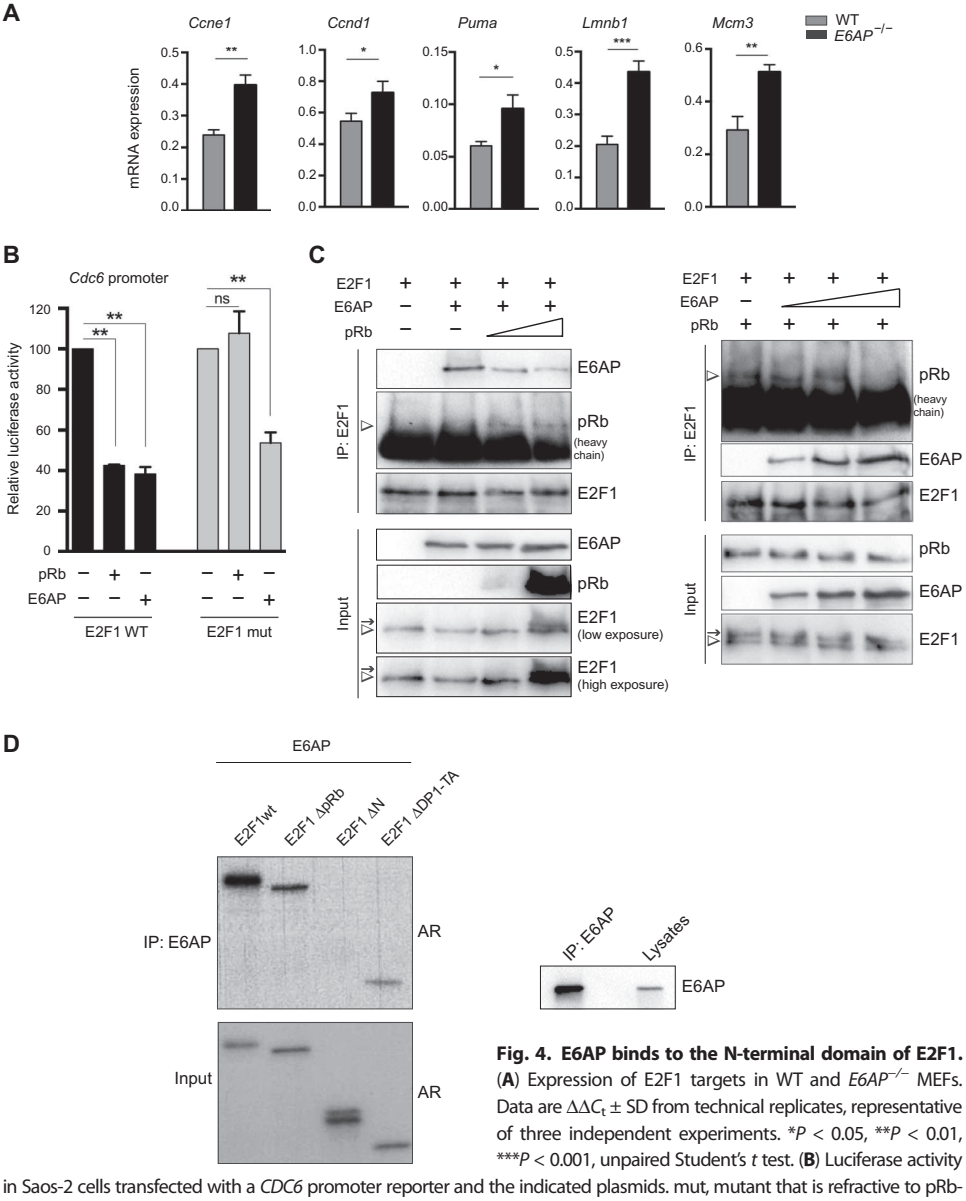

Fig. 4. E6AP binds to the N-terminal domain of E2F1. (**A**) Expression of E2F1 targets in WT and *E6AP*$^{-/-}$ MEFs. Data are $\Delta\Delta C_t \pm$ SD from technical replicates, representative of three independent experiments. *$P < 0.05$, **$P < 0.01$, ***$P < 0.001$, unpaired Student's *t* test. (**B**) Luciferase activity in Saos-2 cells transfected with a *CDC6* promoter reporter and the indicated plasmids. mut, mutant that is refractive to pRb-mediated inhibition. Data are means ± SD of biological triplicates, representative of three independent experiments. **$P < 0.01$, Student's *t* test. (**C**) Immunoblot analysis of in vitro competition assays with the indicated purified proteins followed by coimmunoprecipitation with E2F1 antibody. Arrows indicate signal remaining from previous blotting with pRb antibody. Arrowheads indicate the intended signal. Heavy chain IgG detection is noted in the immunoprecipitation pRb blots. Data are representative of three independent experiments. (**D**) E6AP and in vitro–translated [^{35}S]methionine/cysteine-labeled E2F1 WT and truncated mutants were used in an immunoprecipitation assay. E6AP antibodies were used to immunoprecipitate E6AP with the coimmunoprecipitation of radiolabeled WT E2F1 or E2F1 mutants. The presence of each E2F1 mutant was detected by autoradiography (AR). Bottom: Immunoblot shows the efficiency of the E6AP immunoprecipitation. Blots are representative of two independent experiments.

DISCUSSION

The gene products of the *INK4/ARF* locus control the two main tumor suppressor pathways in the cell, the ARF-p53 and the p16^{INK4a}-pRb pathways. Consistently, it is one of the most rearranged loci in human cancers (*2*). Specifically, p16^{INK4a} expression is lost at high frequency in multiple cancer types by different mechanisms: epigenetic regulation of the entire *INK4/ARF* locus, promoter hypermethylation, genetic deletions, or mutation of the p16^{INK4a} gene. Together, these account for ~37% of the cases with p16^{INK4a} silencing; however, for the remaining cases, the mechanisms are unclear.

Here, we identified a novel regulatory pathway, which provides a molecular explanation for the down-regulation of p16^{INK4a} expression (Fig. 6). We found that E6AP inhibits the induction of the *CDC6* promoter by E2F1. Mechanistically, we demonstrated that E6AP regulates *CDC6* transcription by reducing the ability of E2F1 to bind to *CDC6* promoter. The extent by which E2F1 activity was inhibited by E6AP was comparable to that achieved by pRb, the key inhibitor of E2F1 during the cell cycle (*31*). We showed that E6AP interacted with the N-terminal region of E2F1 (Fig. 4D and fig. S5). Strikingly, pRb binds E2F1 in two regions: at the C-terminal (to regulate its cell cycle role) and at the N-terminal region (to mediate its cytotoxic response to stress) (*40*). Interaction through both regions reduces the binding of E2F1 to DNA, presumably through conformational change induced by the binding. Therefore, E6AP and pRb share the same binding site at the N-terminal region, which provide molecular explanation for the competition for E2F1 binding

(Fig. 4C). It also suggests that the interaction of E6AP with the N-terminal region of E2F1 affects its binding to DNA in a similar manner to pRb, that is, through conformational change (*40*). Moreover, E6AP inhibited E2F1 in pRb-deficient cells (Saos-2), and an E2F1 mutant that is refractory to inhibition by pRb through the C terminus was inhibited by E6AP. We therefore concluded that the inhibition of E2F1 by E6AP is pRb-independent and hence is unlikely to be cell cycle–dependent. Because the interaction of pRb with the N-terminal region of E2F1 is induced by stress, it is possible that E6AP interacts with the N-terminal region of E2F1 in response to different stress conditions, such as oxidative or oncogenic stress (*29*, *30*). This interaction of E6AP with N-terminal E2F1 reduces its DNA binding, and hence its activity presumably through conformational change as proposed for pRb (*40*).

Loss of $p16^{INK4a}$ or increased *CDC6* expression in NSCLC patients is linked to poor prognosis of NSCLC patients (*4*, *8*, *9*, *36*). This prompted us to test the involvement of the E6AP-CDC6-$p16^{INK4a}$ axis in NSCLC, which revealed a cohort of NSCLC patients (18%) with E6AP-low/CDC6-high/$p16^{INK4a}$-low expression profile. Only a small percentage of patients with this expression profile exhibit $p16^{INK4a}$ methylation, supporting our notion that the E6AP-CDC6 axis represents a methylation-independent mechanism of $p16^{INK4a}$ suppression. This cohort presents the worst overall survival and predicts the prognostic value for this expression profile. This proposition gained support by mining a publicly available data set from Kaplan-Meier Plotter, which revealed that low *E6AP* expression predicts poorer survival for lung cancer patients at the early disease stage. Surprisingly, this difference was observed in lung adenocarcinoma patients but not in squamous cell carcinoma patients. One possible contributor to this disparity is the strong association between E6AP-low/CDC6-high/$p16^{INK4a}$-low expression profile and KRAS, the common oncogenic driver in adenocarcinoma patients (>3-fold over the control group). This link is consistent with our previous study demonstrating the cooperativity between activated RAS and loss of E6AP in bypassing cellular senescence (*29*). It would be interesting to test the involvement of the E6AP/CDC6/p16 pathway in other RAS-driven diseases. Our results unravel the predictive value of the E6AP-low/CDC6-high/$p16^{INK4a}$-low expression profile in NSCLC and indicate novel opportunities to therapeutically restore tumor suppression by p16 in NSCLC.

In addition to our finding of low E6AP protein abundance in NSCLC, other studies have also shown low expression of E6AP mRNA in lung adenocarcinomas (figs. S8 and S9), although at low frequency, suggesting that at least in part this down-regulation occurs at the protein level. Low E6AP expression has also been observed in triple-negative breast cancer, where it is associated with poorer survival (*18*). Similarly, albeit by different mechanisms, normal E6AP function is compromised in HPV-infected cells. The E6 protein of the high-risk HPV redirects E6AP to the destruction of the

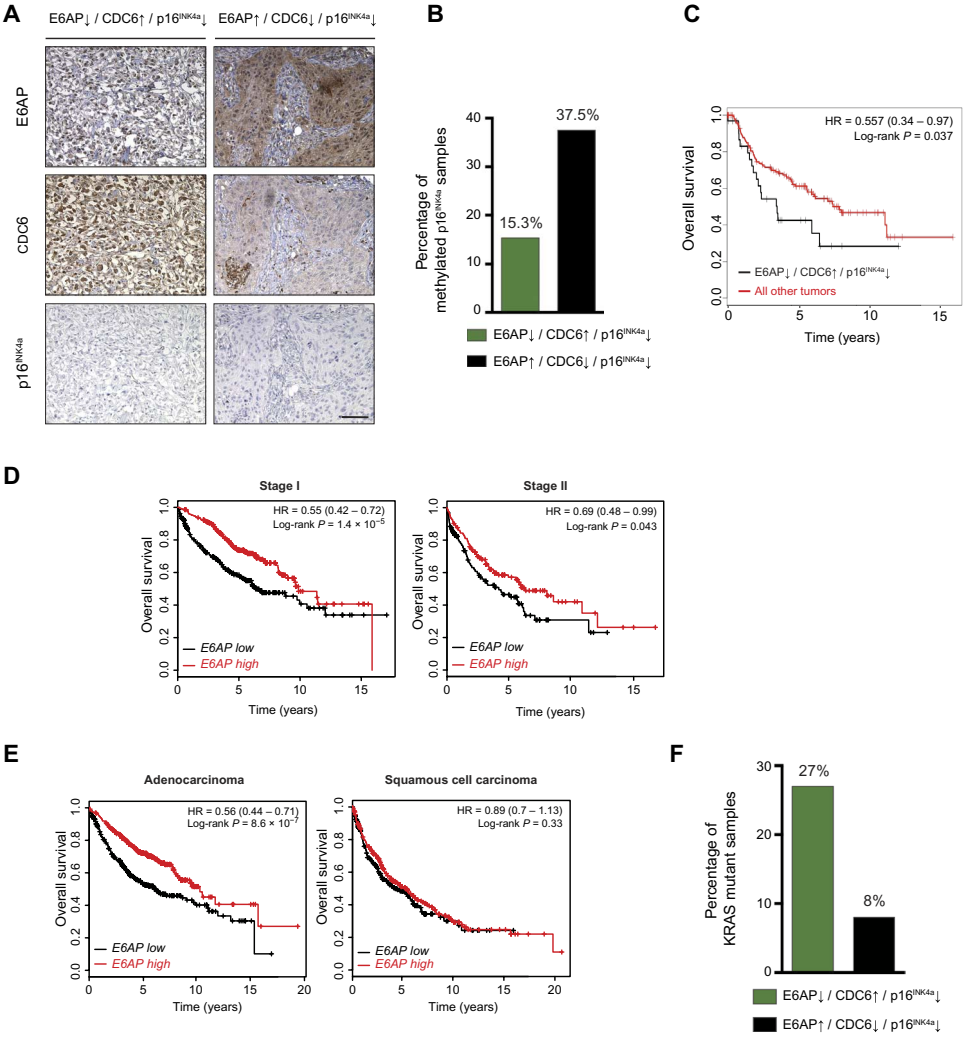

Fig. 5. E6AP is down-regulated in primary NSCLC patient's samples and is associated with low $p16^{INK4a}$ methylation and poor clinical outcome in lung cancer patients. (**A**) Representative images of primary human NSCLC TMA stained by immunohistochemistry for E6AP, CDC6, and $p16^{INK4a}$. A subpopulation characterized by E6AP-low/CDC6-high/$p16^{INK4a}$-low is shown on the left, whereas control subpopulation E6AP-high/CDC6-low/$p16^{INK4a}$-low is shown on the right. Scale bar, 100 μm. (**B**) Quantification of percentage of cases with $p16^{INK4a}$ methylation in each of the subpopulations of NSCLC human samples described in (A). (**C**) Kaplan-Meier overall survival analysis of NSCLC cases separated into two groups: E6AP-low/CDC6-high/$p16^{INK4a}$-low and all the other cases (n = 185 patients). HR, hazard ratio. (**D**) Survival curves from patients with stage I (n = 652) or stage II (n = 320) lung cancer stratified by *E6AP* expression. Data obtained from the Kaplan-Meier Plotter database. (**E**) Survival curves from patients with adenocarcinoma (n = 866) and squamous cell carcinoma (n = 675) stratified by *E6AP* expression. Data obtained from the Kaplan-Meier Plotter database. (**F**) Quantification of percentage of cases with oncogenic KRAS mutation in each of the subpopulations of our data set of NSCLC patients described in (A).

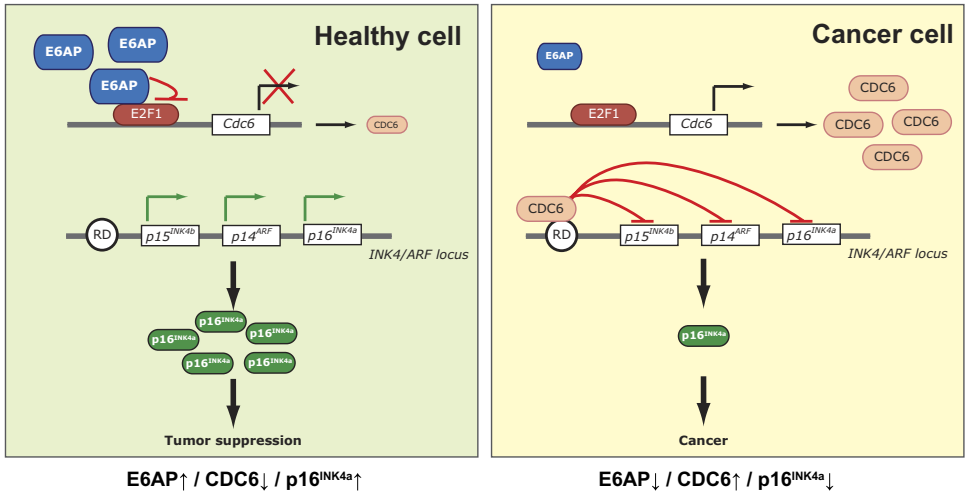

Fig. 6. Model depicting how low abundance of E6AP promotes lung tumorigenesis by silencing $p16^{INK4a}$ in a methylation-independent manner. In a healthy lung tissue, E6AP restricts the abundance of CDC6 by inhibiting E2F1 transcription activity. This results in high $p16^{INK4a}$ amounts that are tumor suppressive in the lung. In cancer cells, low or lost expression of *E6AP* results in high abundance of CDC6, which represses the *INK4/ARF* locus and therefore results in low amounts of $p16^{INK4a}$, which is tumorigenic in the lung. RD, cis-acting regulatory domain.

tumor suppressor p53 (*17*). E6AP also targets another tumor suppressor, the PML (*25*). In this context, E6AP targets PML for degradation in subsets of B cell lymphomas and prostate cancer patients (*19*–*21*).

MATERIALS AND METHODS

Cell culture and reagents

All cell lines except for MEFs were obtained from the America Type Culture Collection. No additional authentication was conducted by the authors. All cells were maintained in Dulbecco's modified Eagle's medium supplemented with 10% fetal bovine serum. MEFs were derived from wild-type and $E6AP^{-/-}$ mice and cultured as described previously (*29*). In all experiments, early-passage MEFs were used (between passages 2 and 5). The reagents used in cellular experiments were the proteasome inhibitor MG132 (474790, Merck), cycloheximide (239764, Calbiochem), and doxycycline (D9891, Sigma).

Plasmids transfections and viral infection

Complementary DNA (cDNA) transfections were carried out as previously described (*30*). Retroviral production and infection to overexpress E6AP was performed as previously described (*29*). For lentiviral infection of Saos-2 cells, a third-generation lentiviral vector, FH1t with green fluorescent protein (GFP) tag (*41*) was used to generate short hairpin RNA (shRNA) to knock down E6AP and for the wobble control consisting of the same sequence as the short hairpin against E6AP but with three nucleotides substituted (underlined) so it does not induce E6AP knockdown. The primer sequences are detailed in table S1. Ten micrograms of FH1t-shE6AP or FH1t-shWobble was transfected along with the appropriate lentivirus packaging plasmids into HEK293T cells, and several batches of the supernatants were collected up to 72 hours after transfection. Saos-2 cells were incubated with the concentrated viral particles (250 μl) in the presence of polybrene (8 μg/ml; H9268, Sigma) for 6 hours. Seventy-two hours after infection, cells were sorted on the basis of the expression of reporter GFP (Becton Dickinson FACSAria II flow cytometer). E6AP downregulation was achieved by treatment of the cells with doxycycline (0.2 μg/ml) for at least 3 days.

RNA extraction and qRT-PCR

RNA was isolated using TRIzol reagent (Life Technologies) in accordance with the manufacturer's instructions. cDNA was synthesized using M-MLV reverse transcriptase (Promega) and Random Primers (Promega). PCR was performed on StepOnePlus PCR machine (Applied Biosystems) using Fast SYBR Green Master Mix (Applied Biosystems). The mouse primer sequences are detailed in table S1. Mouse *Ubc* was used as a control. All the assays were performed in technical triplicates in at least three independent experiments.

Protein extraction and Western blot analysis

Cells were lysed with 50 mM tris-HCl (pH 7.4), 250 mM NaCl, 5 mM EDTA, and 0.1% Triton X-100 supplemented with protease and phosphatase inhibitors. Western blots were probed with antibodies against $p16^{INK4a}$ (sc-1207), MEL18 (sc-10744), BMI-1 (sc-10745), CBX2 (sc-19297), CDC6 (sc-9964), E2F1 (sc-193), and pRb (sc-50), each from Santa Cruz Biotechnology; E6AP (E8655), β-tubulin (T2200), and actin (A4700), each from Sigma; RING1B (5694), rabbit IgG light chain (3677), and Myc (2276), each from Cell Signaling Technology; and HA (11867423001) from Roche.

Immunoprecipitation

Cells were lysed in 50 mM tris-HCl (pH 8), 150 mM NaCl, 5 mM EDTA, and 0.5% NP-40 supplemented with protease and phosphatase inhibitors. For each immunoprecipitation assay, 1 mg of total cell lysates was used. Protein lysates were precleared with protein A/G agarose beads (Calbiochem) for 1 hour and then incubated with 1 μg of the appropriate antibody [E2F1 (sc-193, Santa Cruz Biotechnology), E6AP (E8655, Sigma), or IgG control (sc-2027, Santa Cruz Biotechnology)] overnight at 4°C with orbital rotation followed by incubation with protein A/G agarose beads or protein A/G dynabeads for 1 hour and washed four times in 50 mM tris (pH 8), 150 mM NaCl, 5 mM EDTA, and 0.1% NP-40 supplemented with protease and phosphatase inhibitors. Proteins were eluted from the beads with SDS–β-mercaptoethanol sample buffer, boiled for 10 min, and detected by Western blotting as described above.

For in vitro immunoprecipitation assays, purified E6AP and E2F1 recombinant proteins were used following the same protocol. For E6AP and E2F1 recombinant protein production, codon-optimized full-length E6AP (accession number Q05086) and E2F1 (Q01094) were cloned into a modified pET43 vector with an N-terminal His-tag, and proteins were purified using Ni–immobilized metal affinity chromatography resin (Roche) followed by size exclusion chromatography.

The E2F1 wild type and the truncated mutants [E2F1 ΔpRb (Δ401–437), E2F1 ΔN (Δ1–198), and E2F1 ΔDP1-TA (Δ192–437)] used in Fig. 4D and fig. S5 were a gift from X. Lu. E2F1 wild type and the truncated mutants were in vitro translated and labeled (when required) with S35M or S35C using the TNT T7 Quick Coupled transcription-translation system (Promega) following the manufacturer's

instructions. Immunoprecipitation was performed as detailed above with either a cocktail of antibodies specific for E6AP (E8655, Sigma; MCA3532Z, Serotec; and sc-25509, Santa Cruz Biotechnology) or an antibody specific for Myc (2276, Cell Signaling). Detection was done either by autoradiography or immunoblotting using the indicated antibodies.

Competition assay

For the in vitro competition assays, E6AP, E2F1, and pRb_{ABC} were purified as detailed above. Purified proteins were resuspended in 100 µl of 50 mM tris (pH 8), 150 mM NaCl, 5 mM EDTA, and 0.1% NP-40 supplemented with protease inhibitors and incubated for 30 min in agitation at room temperature followed by 2 hours at 4°C. The proteins were then immunoprecipitated with an antibody raised in rabbit against E2F1 (sc-193, Santa Cruz Biotechnology) for 4 hours at 4°C in agitation followed by incubation with protein A/G agarose beads for 40 min. Bound proteins were washed four times in 50 mM tris (pH 8), 150 mM NaCl, 5 mM EDTA, and 0.1% NP-40 supplemented with protease and phosphatase inhibitors. Proteins were eluted from the beads with SDS–β-mercaptoethanol sample buffer, boiled for 10 min, and detected by Western blotting.

Luciferase assay

Saos-2 cells were seeded in 12-well plates 24 hours before transfection. The following day, cells were cotransfected with a *CDC6* promoter reporter plasmid (provided by K. Ohtani) along with vectors expressing wild-type E2F1, mutant E2F1 (ΔpRb), E6AP or pRb, and an internal control plasmid constitutively expressing *Renilla* luciferase using polyethylenimine (PEI). Luciferase activity was quantified with the Dual-Luciferase/*Renilla* Reporter Assay System (Promega).

Chromatin immunoprecipitation

ChIP was performed as described previously (*42*) using antibodies raised in rabbit against either E2F1 (sc-193, Santa Cruz Biotechnology) or IgG (sc-2027, Santa Cruz Biotechnology) and protein G–coupled magnetic beads (Dynabeads Protein G, Invitrogen). DNA samples were extracted using phenol/chloroform/isoamyl alcohol and precipitated with sodium acetate. PCRs contained 2.5 ng of immunoprecipitated or diluted total input, 1 µM *CDC6* primers (as detailed in table S1), and GoTaq Hot Start Green Master Mix (Promega). After 30 cycles of amplification, PCR products were run on a 2% agarose gel and analyzed by ethidium bromide staining. The abundance of *CDC6* promoter in the immunoprecipitates was also determined by qPCR using the same *CDC6* primers detailed above. ChIP levels are presented as relative to input chromatin and normalized against IgG. The graph is the result of three biological independent experiments.

NSCLC TMA staining and analysis

All studies carried out on human specimens were approved by the Peter MacCallum Cancer Centre Human Ethics Committee. The Melbourne cohort TMAs containing resected samples from 363 lung cancer patients (185 NSCLC samples with low $p16^{INK4a}$ abundance) were collected from St. Vincent's Hospital and Peter MacCallum Cancer Centre between 1996 and 2009. Samples were analyzed and stained for E6AP, CDC6, and $p16^{INK4a}$ using antibodies against CDC6 (1:125 dilution, SC-8341, Santa Cruz Biotechnology), E6AP (1:50 dilution, MCA3532Z, AbD Serotec), $p16^{INK4a}$ (clone E6H4 prediluted, Roche), and E2F1 (1:50 dilution, SC-251, Santa Cruz Biotechnology). Immunohistochemistry slides were semiquantitatively scored for intensity and proportion of tumor cells with staining in the cell nucleus and cytoplasm. Intensity was scored as 0 (none), 1 (weak), 2 (moderate), or 3 (strong); proportion of cellular staining was scored as a percentage between 0 and 100% in increments of 10. A Histo score (H score) was then determined for each core by multiplying the intensity and proportion scores to give a range of H scores from 0 to 300. Cores were then classified as low (H score, 0 to 149) or high (H score, 150 to 300) based on cytoplasmic staining for CDC6 and both nuclear and cytoplasmic staining for E6AP and $p16^{INK4a}$. Slides were examined on an Olympus FluoView 1000 microscope. Images were analyzed with analySIS software (Soft Imaging System).

DNA methylation analysis of CDKN2A in human samples

The methylation status in the *CDKN2A* promoter region was assessed using the methylation-sensitive high-resolution melting (MS-HRM) methodology as previously described (*43*). All samples were tested in duplicate along with the methylation controls.

Clinical data set analysis

For survival analysis of the Melbourne cohort of NSCLC patients stratified by protein abundance of E6AP, CDC6 and $p16^{INK4a}$ scored as explained above were represented as Kaplan-Meier plots and tested for significance using log-rank tests. For survival analysis using the public data set from Kaplan-Meier Plotter database (*44*), data collection was locked on 16 June 2015. Kaplan-Meier plots and log-rank tests were applied to determine the significance of differences in cumulative survival in lung cancer patients stratified by gene expression of *E6AP* (*UBE3A*). Probe 213291_s_at was used for *UBE3A*.

KRAS mutation analysis of human samples

The KRAS mutation status of the formalin-fixed paraffin-embedded human biopsies was assessed using the MS-HRM methodology as previously described (*45*). Samples with aberrant melting curves were recorded as "mutation-positive" and confirmed with Sanger sequencing.

Statistical analysis

Data are presented as means ± SD or SEM as indicated. The unpaired Student's *t* test was used for comparison between two independent groups. For survival analysis, Kaplan-Meier plots and log-rank tests were applied to determine the significance of differences in cumulative survival. For all statistical comparisons, $P < 0.05$ was considered significant. All statistical analyses were performed using GraphPad Prism (version 7.0a) software. The appropriateness of the statistical tests used has been approved by A. Herschtal, a senior biostatistician at the Peter MacCallum Cancer Centre.

SUPPLEMENTARY MATERIALS

www.sciencesignaling.org/cgi/content/full/10/461/eaaf8223/DC1

Fig. S1. E6AP does not affect *Cdc6* transcript stability.

Fig. S2. Immunoblot of cell lysates from Fig. 3A.

Fig. S3. E3 ligase catalytic activity of E6AP is not required for inhibition of E2F1 transcriptional activity.

Fig. S4. The effect of E6AP on E2F1 targets is specific.

Fig. S5. E6AP binds to the N-terminal domain of E2F1.

Fig. S6. E6AP and pRb inhibit E2F1 transcriptional activity in a nonsynergistic and nonadditive manner.

Fig. S7. Changes in E2F1 abundance did not contribute to the effect of E6AP on *CDC6* expression.

Fig. S8. Low *E6AP* mRNA expression is not associated with clinical outcome in patients with stage III lung cancer.
Fig. S9. Expression of *UBE3A* in lung adenocarcinoma NSCLC patients.
Table S1. List of primers used.

REFERENCES AND NOTES

1. W. Y. Kim, N. E. Sharpless, The regulation of *INK4/ARF* in cancer and aging. *Cell* **127**, 265–275 (2006).
2. C. J. Sherr, *Ink4-Arf* locus in cancer and aging. *Wiley Interdiscip. Rev. Dev. Biol.* **1**, 731–741 (2012).
3. J. Gil, G. Peters, Regulation of the *INK4b-ARF-INK4a* tumour suppressor locus: All for one or one for all. *Nat. Rev. Mol. Cell Biol.* **7**, 667–677 (2006).
4. S. Gonzalez, P. Klatt, S. Delgado, E. Conde, F. Lopez-Rios, M. Sanchez-Cespedes, J. Mendez, F. Antequera, M. Serrano, Oncogenic activity of Cdc6 through repression of the *INK4/ARF* locus. *Nature* **440**, 702–706 (2006).
5. K. Ohtani, A. Tsujimoto, M.-a. Ikeda, M. Nakamura, Regulation of cell growth-dependent expression of mammalian CDC6 gene by the cell cycle transcription factor E2F. *Oncogene* **17**, 1777–1785 (1998).
6. T. G. Petrakis, K. Vougas, V. G. Gorgoulis, Cdc6: A multi-functional molecular switch with critical role in carcinogenesis. *Transcription* **3**, 124–129 (2012).
7. C. Allera-Moreau, I. Rouquette, B. Lepage, N. Oumouhou, M. Walschaerts, E. Leconte, V. Schilling, K. Gordien, L. Brouchet, M. B. Delisle, J. Mazieres, J. S. Hoffmann, P. Pasero, C. Cazaux, DNA replication stress response involving *PLK1, CDC6, POLQ, RAD51* and *CLASPIN* upregulation prognoses the outcome of early/mid-stage non-small cell lung cancer patients. *Oncogenesis* **1**, e30 (2012).
8. P. Karakaidos, S. Taraviras, L. V. Vassiliou, P. Zacharatos, N. G. Kastrinakis, D. Kougiou, M. Kouloukoussa, H. Nishitani, A. G. Papavassiliou, Z. Lygerou, V. G. Gorgoulis, Overexpression of the replication licensing regulators hCdt1 and hCdc6 characterizes a subset of non-small-cell lung carcinomas: Synergistic effect with mutant p53 on tumor growth and chromosomal instability—Evidence of E2F-1 transcriptional control over hCdt1. *Am. J. Pathol.* **165**, 1351–1365 (2004).
9. X. Zhang, D. Xiao, Z. Wang, Y. Zou, L. Huang, W. Lin, Q. Deng, H. Pan, J. Zhou, C. Liang, J. He, MicroRNA-26a/b regulate DNA replication licensing, tumorigenesis, and prognosis by targeting CDC6 in lung cancer. *Mol. Cancer Res.* **12**, 1535–1546 (2014).
10. M. Pinyol, I. Salaverria, S. Bea, V. Fernández, L. Colomo, E. Campo, P. Jares, Unbalanced expression of licensing DNA replication factors occurs in a subset of mantle cell lymphomas with genomic instability. *Int. J. Cancer* **119**, 2768–2774 (2006).
11. C.-J. Feng, H.-J. Li, J.-N. Li, Y.-J. Lu, G.-Q. Liao, Expression of Mcm7 and Cdc6 in oral squamous cell carcinoma and precancerous lesions. *Anticancer Res* **28**, 3763–3769 (2008).
12. L. Bonds, P. Baker, C. Gup, K. R. Shroyer, Immunohistochemical localization of cdc6 in squamous and glandular neoplasia of the uterine cervix. *Arch. Pathol. Lab. Med.* **126**, 1164–1168 (2002).
13. N. Murphy, M. Ring, C. C. Heffron, B. King, A. G. Killalea, C. Hughes, C. M. Martin, E. McGuinness, O. Sheils, J. J. O'Leary, $p16^{INK4A}$, CDC6, and MCM5: Predictive biomarkers in cervical preinvasive neoplasia and cervical cancer. *J. Clin. Pathol.* **58**, 525–534 (2005).
14. Z. Wu, H. Cho, G. M. Hampton, D. Theodorescu, Cdc6 and cyclin E2 are PTEN-regulated genes associated with human prostate cancer metastasis. *Neoplasia* **11**, 66–76 (2009).
15. J. Li, T. J. Knobloch, M. J. Poi, Z. Zhang, A. T. Davis, P. Muscarella, C. M. Weghorst, Genetic alterations of $RD^{INK4/ARF}$ enhancer in human cancer cells. *Mol. Carcinog.* **53**, 211–218 (2012).
16. T. Kishino, M. Lalande, J. Wagstaff, UBE3A/E6-AP mutations cause Angelman syndrome. *Nat. Genet.* **15**, 70–73 (1997).
17. S. Beaudenon, J. M. Huibregtse, HPV E6, E6AP and cervical cancer. *BMC Biochem.* **9** (Suppl. 1), S4 (2008).
18. S. Ramamoorthy, R. Tufail, J. E. Hokayem, M. Jorda, W. Zhao, Z. Reis, Z. Nawaz, Overexpression of ligase defective E6-associated protein, E6-AP, results in mammary tumorigenesis. *Breast Cancer Res. Treat.* **132**, 97–108 (2012).
19. S. E. Birch, J. G. Kench, E. Takano, P. Chan, A.-L. Chan, K. Chiam, A.-S. Veillard, P. Stricker, S. Haupt, Y. Haupt, L. Horvath, S. B. Fox, Expression of E6AP and PML predicts for prostate cancer progression and cancer-specific death. *Ann. Oncol.* **25**, 2392–2397 (2014).
20. S. Srinivasan, Z. Nawaz, E3 ubiquitin protein ligase, E6-associated protein (E6-AP) regulates PI3K-Akt signaling and prostate cell growth. *Biochim. Biophys. Acta* **1809**, 119–127 (2011).
21. K. Wolyniec, J. Shortt, E. de Stanchina, Y. Levav-Cohen, O. Alsheich-Bartok, I. Louria-Hayon, V. Corneille, B. Kumar, S. J. Woods, S. Opat, R. W. Johnstone, C. L. Scott, D. Segal, P. P. Pandolfi, S. Fox, A. Strasser, Y.-H. Jiang, S. W. Lowe, S. Haupt, Y. Haupt, E6AP ubiquitin ligase regulates PML-induced senescence in Myc-driven lymphomagenesis. *Blood* **120**, 822–832 (2012).
22. Y.-h. Jiang, D. Armstrong, U. Albrecht, C. M. Atkins, J. L. Noebels, G. Eichele, J. D. Sweatt, A. L. Beaudet, Mutation of the Angelman ubiquitin ligase in mice causes increased cytoplasmic p53 and deficits of contextual learning and long-term potentiation. *Neuron* **21**, 799–811 (1998).
23. A. Mishra, N. R. Jana, Regulation of turnover of tumor suppressor p53 and cell growth by E6-AP, a ubiquitin protein ligase mutated in Angelman mental retardation syndrome. *Cell. Mol. Life Sci.* **65**, 656–666 (2008).
24. M. Scheffner, B. A. Werness, J. M. Huibregtse, A. J. Levine, P. M. Howley, The E6 oncoprotein encoded by human papillomavirus types 16 and 18 promotes the degradation of p53. *Cell* **63**, 1129–1136 (1990).
25. I. Louria-Hayon, O. Alsheich-Bartok, Y. Levav-Cohen, I. Silberman, M. Berger, T. Grossman, K. Matentzoglu, Y.-H. Jiang, S. Muller, M. Scheffner, S. Haupt, Y. Haupt, E6AP promotes the degradation of the PML tumor suppressor. *Cell Death Differ.* **16**, 1156–1166 (2009).
26. A. Mishra, S. K. Godavarthi, N. R. Jana, *UBE3A*/E6-AP regulates cell proliferation by promoting proteasomal degradation of p27. *Neurobiol. Dis.* **36**, 26–34 (2009).
27. Z. Nawaz, D. M. Lonard, C. L. Smith, E. Lev-Lehman, S. Y. Tsai, M.-J. Tsai, B. W. O'Malley, The Angelman syndrome-associated protein, E6-AP, is a coactivator for the nuclear hormone receptor superfamily. *Mol. Cell. Biol.* **19**, 1182–1189 (1999).
28. L. Sivaraman, Z. Nawaz, D. Medina, O. M. Conneely, B. W. O'Malley, The dual function steroid receptor coactivator/ubiquitin protein-ligase integrator E6-AP is overexpressed in mouse mammary tumorigenesis. *Breast Cancer Res. Treat.* **62**, 185–195 (2000).
29. Y. Levav-Cohen, K. Wolyniec, O. Alsheich-Bartok, A. L. Chan, S. J. Woods, Y. H. Jiang, S. Haupt, Y. Haupt, E6AP is required for replicative and oncogene-induced senescence in mouse embryo fibroblasts. *Oncogene* **31**, 2199–2209 (2012).
30. K. Wolyniec, Y. Levav-Cohen, Y.-H. Jiang, S. Haupt, Y. Haupt, The E6AP E3 ubiquitin ligase regulates the cellular response to oxidative stress. *Oncogene* **32**, 3510–3519 (2012).
31. S. P. Chellappan, S. Hiebert, M. Mudryj, J. M. Horowitz, J. R. Nevins, The E2F transcription factor is a cellular target for the RB protein. *Cell* **65**, 1053–1061 (1991).
32. W. Krek, D. M. Livingston, S. Shirodkar, Binding to DNA and the retinoblastoma gene product promoted by complex formation of different E2F family members. *Science* **262**, 1557–1560 (1993).
33. B. Xiao, J. Spencer, A. Clements, N. Ali-Khan, S. Mittnacht, C. Broceño, M. Burghammer, A. Perrakis, R. Marmorstein, S. J. Gamblin, Crystal structure of the retinoblastoma tumor suppressor protein bound to E2F and the molecular basis of its regulation. *Proc. Natl. Acad. Sci. U.S.A.* **100**, 2363–2368 (2003).
34. A. M. Groeger, M. Caputi, V. Esposito, A. De Luca, L. Bagella, C. Pacilio, W. Klepetko, G. G. Giordano, F. Baldi, H. E. Kaiser, E. Wolner, A. Giordano, Independent prognostic role of p16 expression in lung cancer. *J. Thorac. Cardiovasc. Surg.* **118**, 529–535 (1999).
35. W. Sterlacci, A. Tzankov, L. Veits, B. Zelger, M. P. Bihl, A. Foerster, F. Augustin, M. Fiegl, S. Savic, A comprehensive analysis of p16 expression, gene status, and promoter hypermethylation in surgically resected non-small cell lung carcinomas. *J. Thorac. Oncol.* **6**, 1649–1657 (2011).
36. S. Vonlanthen, J. Heighway, M. P. Tschan, M. M. Borner, H. J. Altermatt, A. Kappeler, A. Tobler, M. F. Fey, N. Thatcher, W. G. Yarbrough, D. C. Betticher, Expression of p16INK4a/p16α and p19ARF/p16β is frequently altered in non-small cell lung cancer and correlates with p53 overexpression. *Oncogene* **17**, 2779–2785 (1998).
37. R. González-Quevedo, C. García-Aranda, A. Morán, C. De Juan, A. Sánchez-Pernaute, A. Torres, E. Díaz-Rubio, J.-L. Balibrea, M. Benito, P. Iniesta, Differential impact of p16 inactivation by promoter methylation in non-small cell lung and colorectal cancer: Clinical implications. *Int. J. Oncol.* **24**, 349–355 (2004).
38. The Cancer Genome Atlas Research Network, Comprehensive molecular profiling of lung adenocarcinoma. *Nature* **511**, 543–550 (2014).
39. Y. Sekido, K. M. Fong, J. D. Minna, Molecular genetics of lung cancer. *Annu. Rev. Med.* **54**, 73–87 (2003).
40. F. A. Dick, N. Dyson, pRB contains an E2F1-specific binding domain that allows E2F1-induced apoptosis to be regulated separately from other E2F activities. *Mol. Cell* **12**, 639–649 (2003).
41. M. J. Herold, J. van den Brandt, J. Seibler, H. M. Reichardt, Inducible and reversible gene silencing by stable integration of an shRNA-encoding lentivirus in transgenic rats. *Proc. Natl. Acad. Sci. U.S.A.* **105**, 18507–18512 (2008).
42. T. I. Lee, S. E. Johnstone, R. A. Young, Chromatin immunoprecipitation and microarray-based analysis of protein location. *Nat. Protoc.* **1**, 729–748 (2006).
43. A. M. Lim, H. Do, R. J. Young, S. Q. Wong, C. Angel, M. Collins, E. A. Takano, J. Corry, D. Wiesenfeld, S. Kleid, E. Sigston, B. Lyons, S. B. Fox, D. Rischin, A. Dobrovic, B. Solomon, Differential mechanisms of *CDKN2A* (p16) alteration in oral tongue squamous cell carcinomas and correlation with patient outcome. *Int. J. Cancer* **135**, 887–895 (2014).
44. B. Győrffy, P. Surowiak, J. Budczies, A. Lánczky, Online survival analysis software to assess the prognostic value of biomarkers using transcriptomic data in non-small-cell lung cancer. *PLOS ONE* **8**, e82241 (2013).

45. H. Do, M. Krypuy, P. L. Mitchell, S. B. Fox, A. Dobrovic, High resolution melting analysis for rapid and sensitive EGFR and *KRAS* mutation detection in formalin fixed paraffin embedded biopsies. *BMC Cancer* **8**, 142 (2008).

Acknowledgments: We thank L. Lambeth, M. Herold, X. Lu, and K. Ohtani for gifts of plasmids. We thank K. Hale and L. Dawes for technical support. **Funding:** This work was supported by grants from the National Health and Medical Research Council (NHMRC) of Australia to Y.H. (NHMRC 1063389 and 1026990), by a grant from the Cancer Council Victoria (1085154), and by the Victorian Endowment for Science, Knowledge, and Innovation award. C.G. was supported by a Victorian Cancer Agency–Richard Pratt Fellowship (Pratt14002). **Author contributions:** C.G., S.H., and Y.H. conceived and designed the study and wrote and revised the manuscript. C.G., Y.L.-C., T.G., R.J.Y., H.D., E.T., P.R., and G.W. developed the methodology. P.P., N.W., S.B.F., D.G., B.J.M., and A.D. acquired the data. C.G., S.H., B.S., and Y.H. analyzed and interpreted the data. C.G., P.R., G.W., and Y.H. provided administrative, technical, or material support. Y.H. supervised the study. **Competing interests:** The authors declare that they have no competing interests. **Data and materials availability:** A material transfer agreement is required to obtain the E6AP (*Ube3a*) knockout fibroblasts.

Submitted 5 April 2016
Accepted 7 December 2016
Published 10 January 2017
10.1126/scisignal.aaf8223

Citation: C. Gamell, T. Gulati, Y. Levav-Cohen, R. J. Young, H. Do, P. Pilling, E. Takano, N. Watkins, S. B. Fox, P. Russell, D. Ginsberg, B. J. Monahan, G. Wright, A. Dobrovic, S. Haupt, B. Solomon, Y. Haupt, Reduced abundance of the E3 ubiquitin ligase E6AP contributes to decreased expression of the *INK4/ARF* locus in non–small cell lung cancer. *Sci. Signal.* **10**, eaaf8223 (2017).

Science Signaling

Reduced abundance of the E3 ubiquitin ligase E6AP contributes to decreased expression of the *INK4/ARF* locus in non–small cell lung cancer

Cristina Gamell, Twishi Gulati, Yaara Levav-Cohen, Richard J. Young, Hongdo Do, Pat Pilling, Elena Takano, Neil Watkins, Stephen B. Fox, Prudence Russell, Doron Ginsberg, Brendon J. Monahan, Gavin Wright, Alex Dobrovic, Sue Haupt, Ben Solomon and Ygal Haupt

Sci. Signal. **10** (461), eaaf8223.
DOI: 10.1126/scisignal.aaf8223

***INK4/ARF* repression in lung cancer by loss of E6AP**

The abundance of the cell cycle decelerator $p16^{INK4a}$, encoded at the *INK4/ARF* locus, is decreased in various cancers. Gamell *et al*. found that the absence of $p16^{INK4a}$ in some patients is explained by the lack of the E3 ubiquitin ligase E6AP. E6AP bound to and inhibited the activity of transcription factor E2F1; a decrease in E6AP abundance enabled E2F1-mediated expression of the cell cycle promoter *CDC6*, which encodes a transcriptional regulator that represses *INK4/ARF* expression. The findings identify a tumor-suppressive role for E6AP in lung cancer and suggest that targeting the E2F1-CDC6 pathway might slow tumor growth in some NSCLC patients.

Science Signaling (ISSN 1937-9145) is published by the American Association for the Advancement of Science, 1200 New York Avenue NW, Washington, DC 20005. The title *Science Signaling* is a registered trademark of AAAS.